

Cyclic Spectral Analysis of Fluctuations in a GCM Simulation

JIAN-PING HUANG* AND GERALD R. NORTH

Climate System Research Program, Department of Meteorology, Texas A&M University, College Station, Texas

(Manuscript received 9 February 1995, in final form 6 July 1995)

ABSTRACT

Due to the variety of periodic or quasi-periodic deterministic forcings (e.g., diurnal cycle, seasonal cycle, Milankovitch cycles, etc.), most climate fluctuations may be modeled as cyclostationary processes since their properties are modulated by these cycles. Difficulties in using conventional spectral analysis to explore the seasonal variation of climate fluctuations have indicated the need for some new statistical techniques. It is suggested here that the cyclic spectral analysis be used for interpreting such fluctuations. The technique is adapted from cyclostationarity theory in signal processing. To demonstrate the usefulness of this technique, a very simple cyclostationary stochastic climate model is constructed. The results show that the seasonal cycle strongly modulates the amplitude of the covariance and spectrum. The seasonal variation of intraseasonal oscillations in the Tropics has also been studied on a zonally symmetric all-land planet in the absence of external forcing. The idealized planet has no ocean, no topography. A 15-year length seasonal run of the atmosphere is analyzed with the NCAR Community Climate Model (CCM2, R15). Analysis of the simulation data indicates the presence of intraseasonal oscillations in the Tropics, which are also localized in the time of year.

Both examples suggest that these techniques might be useful for analysis of fluctuations that exhibit locality in both frequency and season.

1. Introduction

Fluctuations are associated with almost all naturally occurring phenomena in the climate system. A better understanding of these fluctuations may provide the basis to create simplified models of the atmosphere that can be used in the coupled system for long-term runs essential for the study of gradually forced climate change. At present, it is impossible to retain all the atmospheric complexity in such simulations because of limited computing capacity. Even when sufficient computer time is available to implement fully coupled high-resolution models in both the ocean and atmosphere, it is anticipated that the results from simplified models will prove useful in interpretation.

A number of investigators have discovered that climate fluctuations strongly depend on the time of year over a broad frequency range. Lau and Lau (1986) noted that although the eastward propagation of the intraseasonal oscillation modes is present throughout the year, there exists strong modulation of these modes by the seasonal cycle. Madden (1986) and Gutzler and

Madden (1993) found that the intraseasonal oscillation is strongest during winter and weakest during summer. Recent studies have proposed that the irregularities of the interannual fluctuation, El Niño–Southern Oscillation (ENSO), can be viewed as a low-order chaotic process driven by the seasonal cycle (Jin et al. 1994; Tziperman et al. 1994). Further understanding of how the seasonal cycle modulates climate fluctuations demands special efforts in time series analysis.

Due to the variety of periodic or quasi-periodic deterministic forcings (e.g., diurnal cycle, seasonal cycle, Milankovitch cycles, etc.), the climate system is not stationary in time, which means that all the traditional methods related to Fourier spectral decomposition are inappropriate (in spite of their ubiquitous use) except for very special types of analysis such as annual means, etc. To give such cyclostationary processes a more precise meaning one must first establish some method of characterizing the structure of processes, such as spectral estimation; empirical orthogonal representation. Gardner (1986, 1988, 1994) has developed a number of techniques for estimating cyclic covariance and cyclic spectral densities for cyclostationary processes. These techniques have been applied in many other fields (Gardner 1994), such as periodic-system identification, detection, and extraction of modulated signals from corrupted observed data. Recently, considerable attention has been given to applying periodic correlation techniques to the study of climatological time series (Bloomfield et al. 1994; Lund et al. 1995). They introduced a frequency domain test for periodic

* Current affiliation: Department of Physics, University of Toronto, Toronto, Ontario, Canada.

Corresponding author address: Dr. Jian-Ping Huang, Climate System Research Program, Department of Meteorology, Texas A&M University, College Station, TX 77843-3150.

correlation. Several prediction techniques for cyclostationary climate systems have also been developed and applied to the problem of predicting ENSO (Hasselmann and Barnett 1981; Zwiers and von Storch 1990). On the other hand, we have undertaken a systematic study of the eigenfunctions of the covariance kernel and have developed a cyclostationary, empirical orthogonal function representation through introduction of Bloch functions (see appendix). This provides a convenient framework for forced climate signal detection in the presence of cyclostationary noise.

The present paper attempts to employ cyclic spectral analysis to study the seasonal variation of climate fluctuations. This study is partly motivated by the fact that the conventional spectral analysis is dependent on the assumptions of stationarity. We could study the seasonal variation of the spectra by breaking the time series up into segments approximately "locally stationary" such as a season long. Seasonal spectra would then be estimated by Fourier analysis and averaging the squares and products of harmonic coefficients across all years for segments beginning the same day each year. Many segment-averaged spectra could be computed with different starting dates. Comparison of results would reveal any seasonal dependence if it exists. Unfortunately, we do not know, a priori, if and when the spectral characteristics change during the year and, therefore, what are appropriate starting dates. To avoid the necessity of computing many segment-averaged spectra determined from segments starting on different days of the year in a trial-and-error fashion, Madden (1986) has developed a seasonally varying cross-spectral analysis technique. This important technique, however, is based on the assumption of stationarity.

In this paper we attempt to provide an estimate of cyclic spectra from two perspectives. First, estimations are to be obtained from a highly simplified, zero-dimensional, cyclostationary, stochastic climate model. Stochastic climate models have been used for a variety of applications in recent years (e.g., Hasselmann 1976; North and Cahalan 1981; North et al. 1992). In these studies it is assumed that the evolution of a climatological function such as global average surface temperature $T(t)$, is governed by a Langevin-type equation. However, the phenomenological coefficients will in many cases be seasonally variable. Hence, we will introduce here a cyclostationary, stochastic climate model by including a periodic modulation of one of the coefficients in the model's governing equation. We will use the model to demonstrate the usefulness of the cyclic spectral analysis. The second application is to be obtained from a specific GCM simulation. To isolate how the seasonal cycle modulates the fluctuations, the ocean, topography, and any symmetry-breaking sources of forcing are removed from the planet whose atmosphere is being simulated by the GCM. The natural timescale of the climate system is then greatly reduced because of the lack of ocean surfaces. It is hoped

that the analysis so obtained can lead to a better understanding of the response of intraseasonal, low-frequency oscillation to the seasonal solar radiation forcing. The intraseasonal oscillations usually have been considered as essentially self-excited and not caused by external astronomical forcing. However, the phase-locking relationship between intraseasonal and seasonal cycle suggests that intraseasonal variations may also be partially influenced by annual solar forcing.

Section 2 gives the background and basic concepts of the techniques of cyclic spectral analysis used in this study. The readers who have already had such background may skip this section and go directly to section 3, in which the cyclostationary, stochastic climate model and their cyclic spectrum are to be described. Section 4 applies the cyclic spectral analysis to the seasonal variation of intraseasonal oscillation in the Tropics in this specific GCM simulation. In section 5, we present the conclusions including a discussion on the further application of cyclic spectral analysis.

2. Cyclic spectra and cyclic cross spectra

In this section we first briefly review some definitions and basic properties of cyclostationary processes, while introducing cyclic spectra that we have used for our analysis. A comprehensive treatment of cyclostationarity in time series can be found in Gardner (1994), and references therein.

a. Definitions of cyclostationary process

If and only if the moments, such as the ensemble mean $M(t)$ and the covariance $C(t, t + \tau)$, are independent of time, the process $T(t)$ is defined to be stationary. If the mean $M(t)$ and covariance $C(t, t + \tau)$ exhibit periodicity in t , the process $T(t)$ is defined to be a cyclostationary process with period d (Bennett 1958; Gardner and Franks 1975); that is, for all t ,

$$M(t + d) = M(t)$$

$$C(t + d, t + d + \tau) = C(t, t + \tau) \quad (1)$$

for monthly data, $d = 12$, for daily data, $d = 365$, and so on. If the mean $M(t)$ and covariance $C(t, t + \tau)$ exhibit the poly-periods $\{d\} = d_1, d_2, d_3, \dots$, the process $T(t)$ is defined to be a poly-cyclostationary process with periods $\{d\}$. Such cyclostationary processes occur commonly in the climate system due to diurnal or seasonal forcings.

Bennett (1958) perhaps first introduced the term "cyclostationary" to denote this class of processes in his treatment of synchronously timed pulse sequences used in digital data transmission. The first mathematical treatment of these processes was by Gladyshev (1961), although Bennett (1958) discovered their characterizing property in a communication theoretic context. Cyclostationary processes have also been called periodically correlated processes (Hurd 1969), periodically

nonstationary (Markelov 1966; Ogura 1971), and processes with periodic structure (Jones 1964; Jones and Brelsford 1967).

b. Cyclic covariance

Similar to the stationary process, the covariance is given by

$$C(t, t + \tau) = \langle (T(t) - M(t))(T(t + \tau) - M(t)) \rangle, \tag{2}$$

where the angular bracket $\langle \cdot \rangle$ denotes ensemble average. For a cyclostationary process $T(t)$, the covariance is periodic in t for each τ . By the properties of periodic functions this implies that $C(t, t + \tau)$ can be decomposed (for each fixed τ) into a Fourier series with respect to t , as

$$C(t, t + \tau) = \sum_{\alpha} C^{\alpha}(\tau) e^{i2\pi\alpha(t+\tau/2)}, \tag{3}$$

$\alpha = 0, \pm 1/d, \pm 2/d, \dots$

where

$$C^{\alpha}(\tau) = \frac{1}{d} \int_{-d/2}^{d/2} C(t, t + \tau) e^{-i2\pi\alpha(t+\tau/2)} dt, \tag{4}$$

$\alpha = 0, \pm 1/d, \pm 2/d, \dots$

are the Fourier coefficients of the n th harmonic of $2\pi/d$, and $C^{\alpha}(\tau)$ is said to be a cyclic-covariance at cycle frequency α . The α index is called the cycle frequency parameter and ranges over all integer multiples of the fundamental frequency $1/d$. The sine wave $\exp[i2\pi\alpha(t + \tau/2)]$ in the Fourier series introduced here contains a time shift $\tau/2$ so that the discrete-time theory presented here will match the continuous-time theory in which the function $C(t + \tau/2, t - \tau/2)$ is expanded in a Fourier series with unshifted sine wave $\exp(i2\pi\alpha t)$ (Gardner 1986, 1988, 1994).

c. Cyclic spectra

Analogous to the dual time and frequency domains for stationary processes, one can define the seasonally varying spectral density as

$$S(t, f) = \int_{-\infty}^{+\infty} C(t, t + \tau) e^{-i2\pi f\tau} d\tau. \tag{5}$$

It follows from (3) that the seasonally varying spectral density for a cyclostationary process is completely characterized by the cyclic spectral density

$$S(t, f) = \sum_{\alpha} S^{\alpha}(f) e^{i2\pi\alpha t}, \tag{6}$$

where the cyclic spectral density is defined as the Fourier transform of the cyclic-covariance

$$S^{\alpha}(f) = \int_{-\infty}^{+\infty} C^{\alpha}(\tau) e^{-i2\pi f\tau} d\tau. \tag{7}$$

For $\alpha = 0$, the cyclic spectra reduce to conventional spectra, since these represent the stationary time series of annual averages.

d. Cyclic cross spectra

Similar to cyclic spectra, we can introduce the cyclic cross spectra. Consider the cyclostationary signals $T_1(t)$ and $T_2(t)$ with the same periodicity d , the cross-covariance $C_{12}(t, \tau)$ can be expressed (for each fixed τ) as a Fourier series with respect to t , as

$$C_{12}(t, t + \tau) = \sum_{\alpha} C_{12}^{\alpha}(\tau) e^{i2\pi\alpha(t+\tau/2)}, \tag{8}$$

where

$$C_{12}^{\alpha}(\tau) = \frac{1}{d} \int_{-d/2}^{d/2} C_{12}(t, t + \tau) e^{-i2\pi\alpha(t+\tau/2)} dt \tag{9}$$

are the Fourier coefficients at the n th harmonic of $2\pi/d$, and $C_{12}^{\alpha}(\tau)$ is said to be a cyclic cross-covariance at cycle frequency α .

Analogously, the seasonally varying cross-spectral density and cyclic cross-spectra S_{12}^{α} for two cyclostationary signals $T_1(t)$ and $T_2(t)$ are given by

$$S_{12}(t, f) = \sum_{\alpha} S_{12}^{\alpha}(f) e^{i2\pi\alpha t} \tag{10}$$

and

$$S_{12}^{\alpha}(f) = \int_{-\infty}^{+\infty} C_{12}^{\alpha}(\tau) e^{-i2\pi f\tau} d\tau. \tag{11}$$

The seasonally varying coherence squared and phase are thus

$$\text{Coh}^2(t, f) = \frac{P_{12}(t, f)^2 + Q_{12}(t, f)^2}{S_1(t, f)S_2(t, f)} \tag{12}$$

$$\theta_{12}(t, f) = \tan^{-1} \frac{Q_{12}(t, f)}{P_{12}(t, f)}, \tag{13}$$

where the $P_{12}(t, f)$ and $Q_{12}(t, f)$ are the real and imaginary parts of the cross spectrum, respectively. Here $S_1(t, f)$ and $S_2(t, f)$ are the seasonally varying spectra for $T_1(t)$ and $T_2(t)$.

It should be emphasized that essentially all the fundamental results of the theory of cyclic spectral analysis are generalizations of results from the conventional theory of spectral analysis, in the sense that the latter are included as the special case of the former for which the cycle frequency α is zero or the time series is purely stationary (Gardner 1986).

e. Estimation of the cyclic spectrum

If the problem has a priori knowledge of the cycle frequencies of interest, and the number of cycle fre-

quencies is not large, estimation of the cyclic spectrum has a computational cost comparable to the conventional spectral analysis. On the other hand, if the cycle frequencies of interest are unknown, then estimation of cyclic spectrum over the entire bifrequency plane can be required. In this case the computational burden can be much greater than it is for the conventional spectral analysis.

The theory and implementation of cyclic spectrum estimation algorithms has been covered in a number of publications. The basic time and frequency smoothing method of the cyclic spectrum are proposed by Gardner (1986). By itself, the time smoothed cyclic periodogram is not computationally efficient for computing estimates of the cyclic spectrum over large regions of the bifrequency plane. However, modification of the time and frequency-smoothed cyclic periodogram leads to several computationally efficient algorithms. In general, fast Fourier transform (FFT) based time-smoothing algorithms are considered most attractive for computing estimates of the cyclic spectrum over the entire bifrequency plane. Frequency smoothing methods of cyclic spectrum are best for computing estimates of the cyclic spectrum along the lines of constant cycle frequency for moderate values of cycle frequency. A detailed review of estimation of the cyclic spectrum can be found in Roberts et al. (1994), and references therein.

3. Cyclostationary stochastic climate model

The cyclostationary stochastic energy balance model describes the behavior of the global average surface-air temperature anomaly field T and is governed by the following Langevin equation

$$\frac{dT(t)}{dt} + [a + b \cos(\omega_0 t + \phi)]T(t) = F(t), \quad (14)$$

where t is time, a and b are constants, $\omega_0 = 2\pi f_0$, $f_0 = 1/d$ is the fundamental cycle frequency such as annual cycle, and $F(t)$ is (roughly speaking) a white noise function. This is, of course, a very simplified model, which is only intended as a mathematical example. The noise $F(t)$ satisfies

$$\langle F(t) \rangle = 0$$

$$\langle F(t)F(t') \rangle = \sigma_F^2 \delta(t - t'), \quad (15)$$

where the angular brackets mean ensemble average and δ is the Dirac delta function. The formal solution $T(t)$ of the nonhomogeneous, linear, stochastic differential equation (14) can be written (after transients have decayed) as

$$T(t) = e^{-(at+b^*\sin(\omega_0 t+\phi))} \int_{-\infty}^t F(t') e^{(at'+b^*\sin(\omega_0 t'+\phi))} dt', \quad (16)$$

where

$$b^* = \frac{b}{\omega_0}. \quad (17)$$

The integration of Eq. (16) can be performed expanding $e^{(b^*\sin(\omega_0 t+\phi))}$ into a Bessel series:

$$e^{(b^*\sin(\omega_0 t+\phi))} = \sum_{n=-\infty}^{+\infty} i^n I_n(b^*) e^{i n (\omega_0 t + \phi)}, \quad (18)$$

where $I_n(x)$ is the modified Bessel function. Therefore, the covariance function can be represented by the series

$$C(t, t + \tau) = \begin{cases} \sigma_F^2 e^{-a\tau} \sum_{m,n,k=-\infty}^{+\infty} B_{mnk}(b^*) \frac{e^{i\omega_0(m+n-k)t} e^{i\omega_0 n \tau} e^{i\phi(m+n-k)}}{(2a - ik\omega_0)}, & \tau \geq 0 \\ \sigma_F^2 e^{a\tau} \sum_{m,n,k=-\infty}^{+\infty} B_{mnk}(b^*) \frac{e^{i\omega_0(m+n-k)t} e^{i\omega_0(n-k)\tau} e^{i\phi(m+n-k)}}{(2a - ik\omega_0)}, & \tau \leq 0 \end{cases} \quad (19)$$

where

$$B_{mnk}(b^*) = (i)^{m+n+k} I_m(b^*) I_n(b^*) I_k(2b^*). \quad (20)$$

Inserting the expression (19) into (4), we have the cyclic covariance

$$C^\alpha(\tau) = \begin{cases} \sigma_F^2 e^{-a\tau} \sum_{m,n,k=-\infty}^{+\infty} B_{mnk}(b^*) \frac{e^{i\omega_0 n \tau} e^{-i\pi\alpha\tau} e^{i\phi(m+n-k)} \delta((m+n-k)f_0 - \alpha)}{(2a - ik\omega_0)}, & \tau \geq 0 \\ \sigma_F^2 e^{a\tau} \sum_{m,n,k=-\infty}^{+\infty} B_{mnk}(b^*) \frac{e^{i\omega_0(n-k)\tau} e^{-i\pi\alpha\tau} e^{i\phi(m+n-k)} \delta((m+n-k)f_0 - \alpha)}{(2a - ik\omega_0)}, & \tau \leq 0. \end{cases} \quad (21)$$

Using (7), it follows that

$$S^\alpha(f) = \sigma_F^2 \sum_{m,n,k=-\infty}^{+\infty} B_{mnk}(b^*) \frac{e^{i\phi(m+n-k)} \delta((m+n-k)f_0 - \alpha)}{(a - i\omega_0 n + i\pi\alpha + i2\pi f)(a + i\omega_0(n-k) - i\pi\alpha - i2\pi f)}. \quad (22)$$

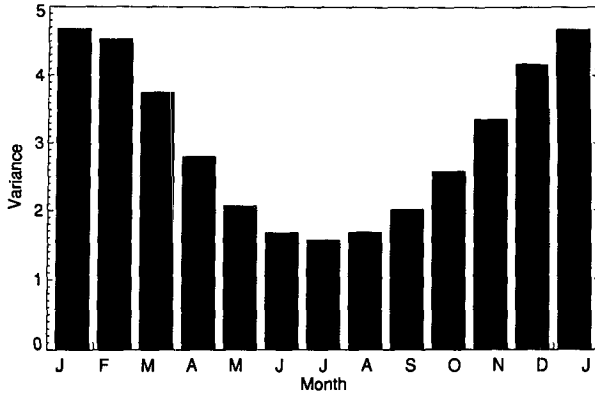


FIG. 1. Variance (autocovariance at time lag $\tau = 0$) of the cyclostationary stochastic climate model.

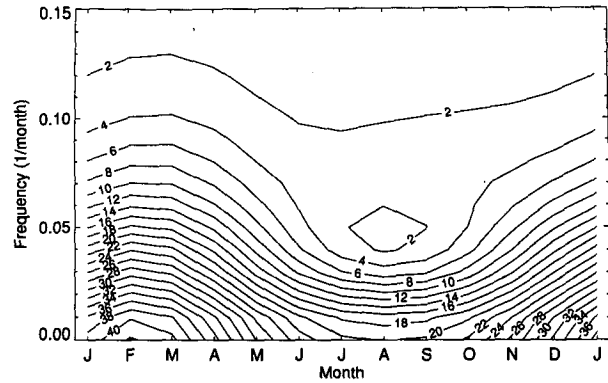


FIG. 2. Seasonal variation of spectra of the cyclostationary stochastic climate model.

As a numerical example for illustration we have chosen $a = 0.2 \text{ mo}^{-1}$, $b = 0.18 \text{ mo}^{-1}$, and $f_0 = 1/d$, where $d = 12 \text{ mo}$, corresponding to the seasonal cycle; $\phi = 72.5^\circ$ is the initial phase; $\sigma_F^2 = 1.0$. Figure 1 shows the variance [i.e., $C(t, 0)$] with this set of values. As can be seen in Fig. 1, the variation of variance with time of year, t , is obviously strong in winter and weak in summer, but for the stationary case ($b = 0$) the variance (or covariance) is independent of seasonal phase. Figure 2 shows the seasonally varying spectra of this model. The spectra decrease with increasing frequency in all months, which can be modeled to a good approximation as a first-order Markov process or ‘‘red noise.’’ The spectra also exhibit a strong seasonal cycle and the seasonal maximum is in February and the minimum spectrum occurs in August. Figure 3 shows the cyclic spectral density for $\alpha = 0$, $\alpha = 1/d$, and $\alpha = 2/d$. The real part of cyclic spectral densities at $\alpha = 0$ (Fig. 3a) is a typical red spectrum as well as the conventional spectral density. The seasonally varying component of cyclic spectral densities (i.e., component at $\alpha = 1/d$) are much stronger than the component at $\alpha = 2/d$. According to Eq. (6), cyclic spectral densities are the Fourier coefficients of seasonally varying spectra. The real and imaginary part of the cyclic spectrum indicate the amplitude and phase of each component. The seasonal variations of the spectra are completely and conveniently characterized by the cyclic spectra $\{S^\alpha\}$. Figures 2 and 3 indicate that this model is strongly modulated by its seasonal cycle.

4. GCM simulation

We have conducted a 15-yr run of a seasonal climate model and will use the output as a further example of our procedures. We used the Community Climate Model version 2 (CCM2), developed at NCAR, that is solved by a spectral method truncated at R15 with 18 vertical levels and is described in detail by Hack et al. (1993). To completely remove the asymmetric and ex-

ternal forcings, we idealized the boundary conditions as follows: 1) the ocean and sea ice were removed, that is, the planetary surface was made to be all land; 2) all topographic features such as mountains were removed to make a zonally symmetric lower boundary at sea

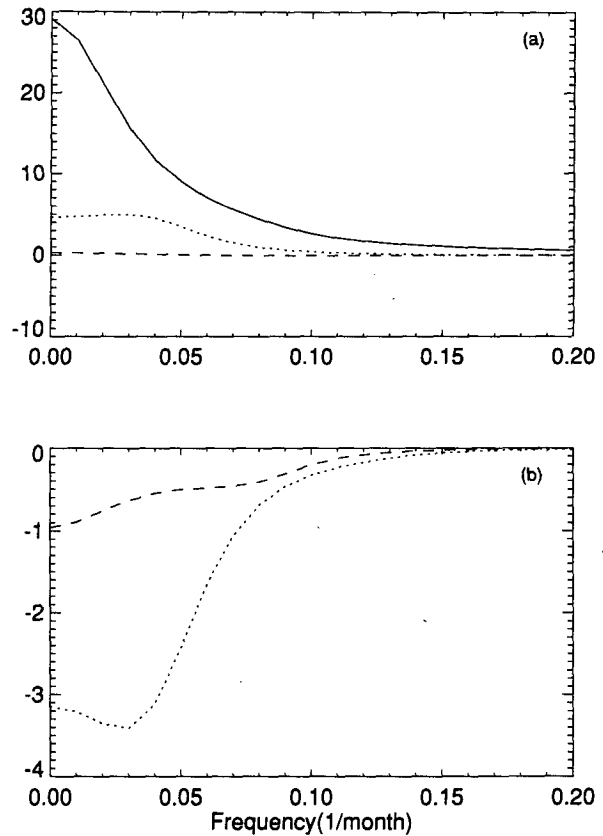


FIG. 3. Cyclic spectra of the cyclostationary stochastic climate model: (a) real part of cyclic spectral density; (b) imaginary part of cyclic spectral density. Solid line for $\alpha = 0$, short-dash line for $\alpha = 1/d$, and long-dash line for $\alpha = 2/d$, $d = 12 \text{ mo}$.

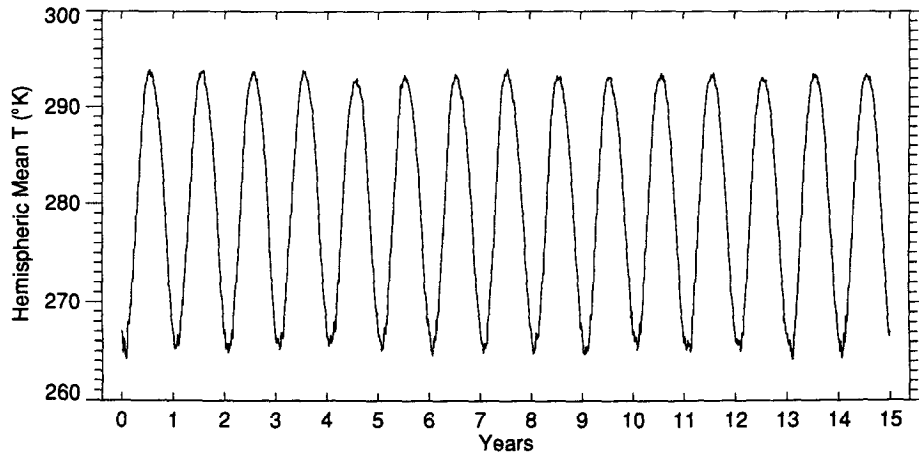


FIG. 4. Hemispherically averaged daily surface temperature for the 15-yr simulation.

level; 3) the surface albedo for the visible spectrum was taken as 0.1 over all land and for the near-infrared spectrum 0.25 over both strong zenith-angle-dependent surfaces and weak zenith-angle-dependent surfaces. The

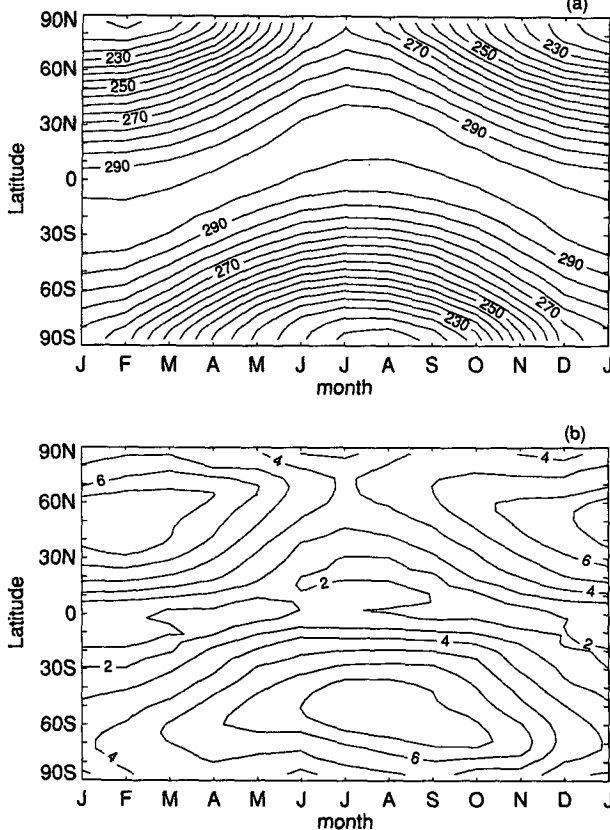


FIG. 5. The seasonal variation of simulation climate: (a) zonal-mean surface temperature; (b) the zonal-mean of the standard deviation of surface temperature.

only latitudinal variation of surface albedo was due to zenith angle. Snow was also removed, so there was no snow-albedo feedback; 4) other surface parameters were simply taken as constant over all land; such as, evaporation factor (soil wetness factor) 0.25, vegetation type 5 (shrubland), aerodynamic roughness 0.4 m; 5) the ozone distributions were prescribed as zonally symmetric, reflection symmetric about the equator and fixed in time. The ozone volume mixing ratios were taken as the annual average of the Northern Hemisphere. This model planet is called *Terra Blanda* and simulations of its atmosphere at perpetual equinox with CCM0 have been discussed in some detail elsewhere (Leung and North 1991; North et al. 1992; Yip and North 1993; North et al. 1993). In this experiment, we introduce the seasonal cycle to our simplified model. The declination angle will vary from -11.75° to 11.75° over one year (half the range for earth), so that the solar heating passes through identical, successive seasonal cycles; thus, no interannual variability will be introduced to the external forcing of the model environment. We need the weaker seasonal forcing to prevent an excessive seasonal cycle on the all-land planet.

Figure 4 presents the 15-yr daily hemispherically averaged surface temperature. The time series shows 15 annual cycles with the minima in December–January–February (DJF) and maxima in June–July–August (JJA). The seasonal variability is much stronger than the interannual variability. The major features of the observed seasonal cycle are captured by the model. Figure 5a shows a well-defined seasonal cycle of the zonal-mean surface temperature. Comparing the variation in one hemisphere with that in the other hemisphere after shifting its phase by a half year, we find that they are quite symmetrical with respect to the equator. In the equatorial region, the seasonal variations are very small because the solar irradiation does not change substantially throughout the year. In middle and high latitudes,

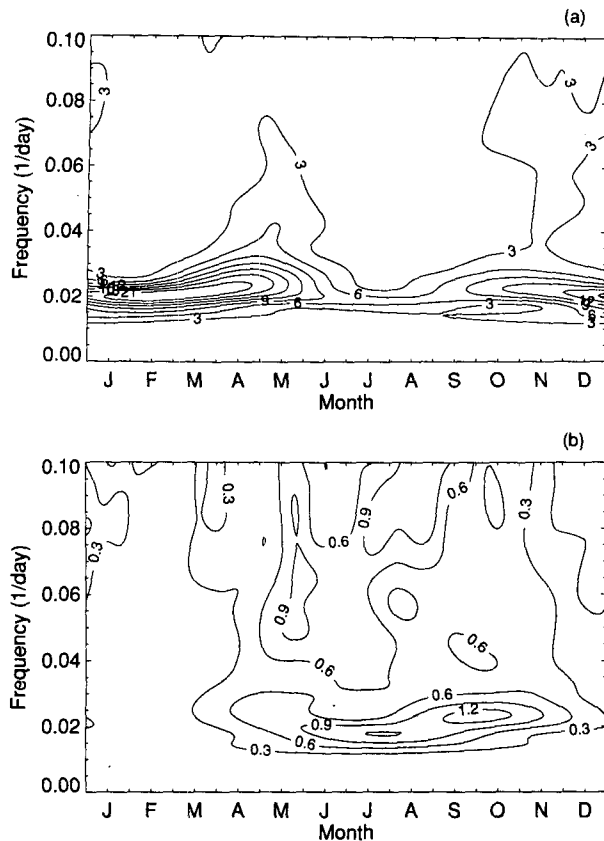


FIG. 6. The seasonally varying spectra for the zonal wind u at (a) 189 hPa; (b) 866 hPa.

a variation with a period of 1 yr is dominant. Figure 5b shows the seasonal variation of zonal-mean standard deviation of the surface temperature. As expected, the variability exhibits a strong seasonal cycle and is larger in the winter hemisphere especially over middle and high latitudes.

Next we apply the cyclic spectral analysis techniques to the fluctuations in the Tropics in this specific simulation. Since the simulation climate is north-south symmetric and longitudinal location makes no difference in the climate, the spectral estimate is not sensitive for using data from different longitudes or from both sides of the equator. The data we use here are latitudinally averaged over 2.2°N to 20°N at the longitudinal location 180° . The data were normalized to remove the seasonal cycle. The climatological seasonal cycles were averaged by the data over 15 yr for each day of the year. The algorithm used for computing estimates of cyclic spectra is the FFT accumulation method. For details of the algorithm, the reader is referred to Roberts et al. (1994).

Figure 6 shows the seasonally varying spectra for the zonal wind at 189 and 866 hPa. There are obvious oscillations with a 40–50 day period (frequency ~ 0.02

d^{-1}) with significant seasonal variability. Figure 6 indicates that, for the 189-hPa u , the spectrum in the 50-day band has a relative maximum from December through May, whereas that for the 866-hPa u has a relative maximum from July through November. As a comparison, Fig. 7 shows the conventional spectral density of the zonal wind u , at 189 hPa. A very prominent peak stands out at the 50-day period. The conventional spectral analysis does yield a distribution of oscillation, but clearly it is unable to provide information on season-frequency localization consistent with the cyclic spectral analysis. Figure 8 shows the seasonally varying coherence squared and phase difference between 189- and 866-hPa u . From Fig. 8 we infer that the 189- and 866-hPa u winds are coherent in 30–70 day bands in all months except March and April. In all months, the phase is larger than 0.5 cycle, and the 866-hPa u tends to be out of phase with the 189-hPa u in 50-day bands. It is consistent with that found by observational studies (e.g., Madden 1986).

Based on an analysis of the fluctuations occurring in the NCAR CCM0 with the same simplified boundary conditions mentioned as above, Yip and North (1993) suggested that an intraseasonal wavelike oscillation may be generated by the internal dynamics of the model instead of being directly forced by imposed boundary conditions. However, the phase-locking relationship between intraseasonal and annual variation suggests that intraseasonal variation may also be modulated by the seasonal cycle through one or more seasonal-dependent energy sources.

In earlier studies (Madden and Julian 1971, 1972), no peaks were found in the v -wind spectra as pronounced as those in the u -wind spectra at 40–50 day periods. On the other hand, both theoretical and simulation studies indicate that convective forcing near the equator, which we presume to be important in the 40–50 day oscillation, excites Rossby waves as well as Kelvin waves. The Rossby waves have v -wind pertur-

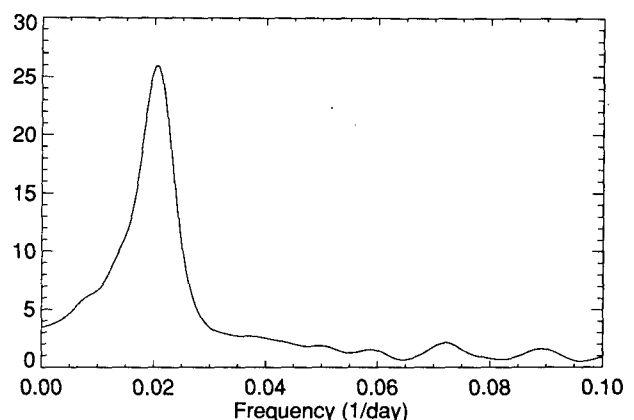


FIG. 7. The conventional spectral density of the zonal wind u at 189 hPa.

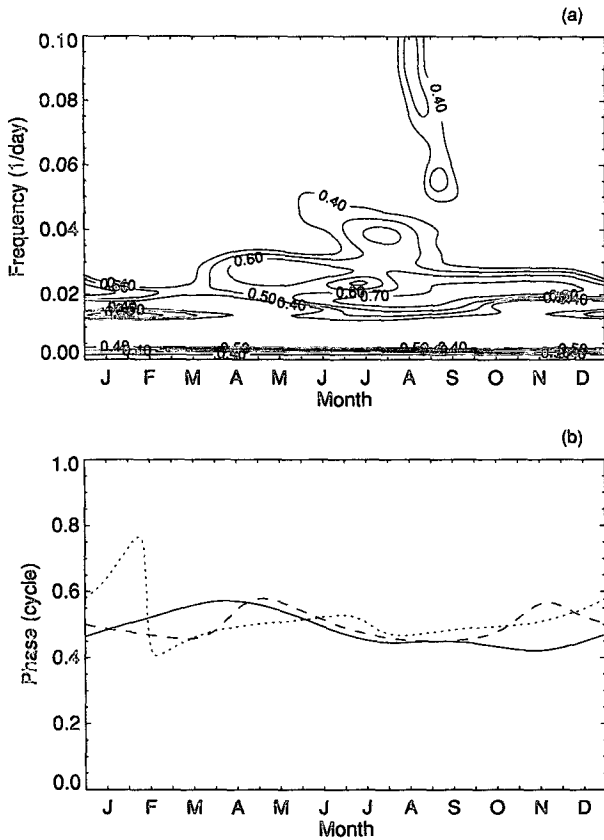


FIG. 8. The seasonally varying coherence squared (a) and phase (b) between 189- and 866-hPa u . Contour interval is 0.1 for coherence squared. Phase is in fractions of a cycle. Phase between 0 and 0.5 means 866-hPa u leads. Solid line is for the phase at frequency of 50-day period, short-dash line for 40-day period, and long-dash line for 60-day period.

bations of comparable magnitude to that of the u -wind perturbation (Yip and North 1993). These results led us to compute seasonally varying spectra for v -wind and cross spectra between u wind and v wind to see if they could shed more light on the role of the v wind.

Figure 9 shows the seasonally varying spectra for the meridional wind at 189 hPa. There is a weak peak in 40–50 day frequency from December through May. It reveals why conventional spectral analysis that averages over all seasons cannot detect this weak peak. Figure 10 shows the seasonally varying coherence squared and phase between 189-hPa u and 189-hPa v . The 189-hPa u and 189-hPa v winds are at least coherent in 50-day frequency bands during winter. The seasonally varying coherence squares exceed 0.8 in 50-day bands in January. In general, the u and v are out of phase, and although phase angle changes, there is no clear cut phase shift between winter and summer.

5. Conclusions and discussions

In this paper we provide the basic framework and some examples of an application of cyclic spectral

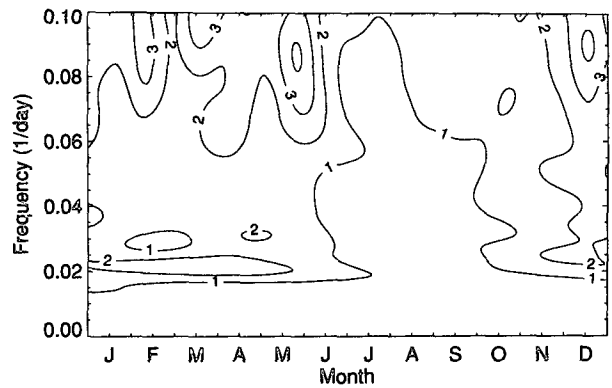


FIG. 9. The seasonally varying spectra for the meridional wind v at 189 hPa.

analysis to climate fluctuation. A process is said to exhibit cyclostationarity in the wide sense if its time-variant covariance $C(t, t + \tau)$ is periodic in t for each τ .

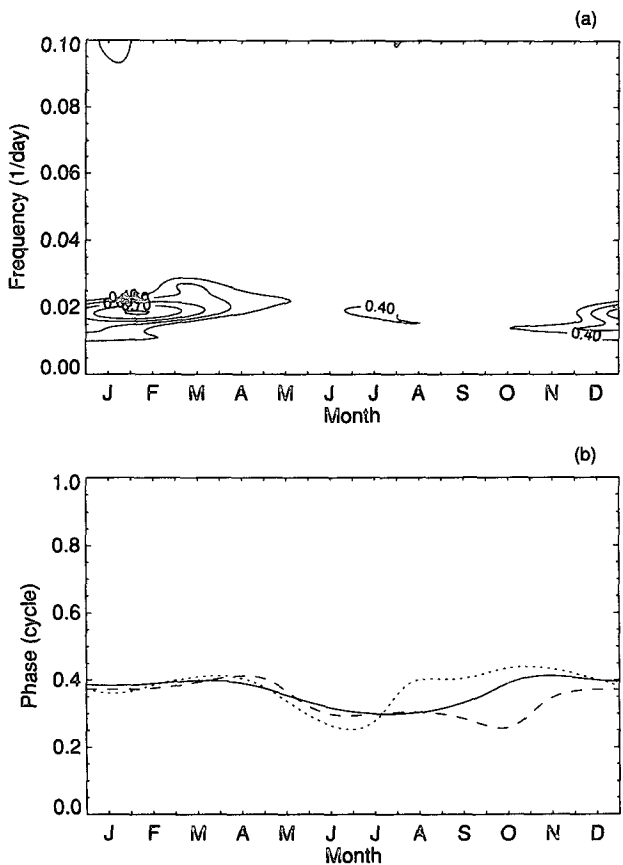


FIG. 10. The seasonally varying coherence squared (a) and phase (b) between 189-hPa u and 866-hPa v . Contour interval is 0.1 for coherence squared. Phase is in fractions of a cycle. Phase between 0 and 0.5 means 189-hPa v leads. Solid line is for the phase at frequency of 50-day period, short-dash line for 40-day period, and long-dash line for 60-day period.

Such processes occur commonly in the climate system due to the variety of periodic or quasi-periodic deterministic forcings (e.g., diurnal cycle, seasonal cycle, 11-yr cycle, Milankovitch cycles, etc.). We have analyzed the cyclic spectra of a cyclostationary stochastic climate model. Our results show a strong seasonal modulation in the covariance and time-varying spectra with respect to time of year. We have also presented the cyclic spectral analysis of the intraseasonal oscillation taken from a long seasonal run with a general circulation model (CCM2-R15) that has simplified boundary conditions. Analysis of the simulation data indicates the presence of intraseasonal oscillations in the Tropics, which are also localized according to time of year. The strength of the intraseasonal oscillations in the upper troposphere is strongest during DJF and weakest during JJA, whereas for the lower troposphere they are strongest during SON. These results suggest that intraseasonal oscillations may be generated by the internal dynamics of the model instead of being directly forced by imposed boundary conditions. However, the phase-locking relationship between intraseasonal and annual variation suggests that intraseasonal variation may also be modulated by the seasonal cycle through one or more seasonally dependent energy sources.

Both examples suggest that these techniques might be useful for analysis of fluctuations that exhibit locality in both frequency and season. The seasonal variations are completely and conveniently characterized by the cyclic spectra. Our characterization of the variations contains more information than the conventional spectral estimate, which results from considering cyclostationary data as being stationary.

Another application of this technique is to detect and classify the multiple fluctuations buried in noise. The essence of the difference between stationary and cyclostationary processes is that the latter exhibit spectral correlation. The existence of correlation between widely separated spectral components can be interpreted as *spectral redundancy*. The distinctive character of spectral redundancy makes signal detection and classification possible. Specifically, for the composite signal

$$T(t) = \sum_l^L T_l(t) + n(t), \quad (23)$$

where the set $\{T_l(t)\}$ includes both signals of interest and interference and where $n(t)$ is background noise, we have the cyclic spectral

$$S_T^\alpha(f) = \sum_l^L S_{T_l}^\alpha(f) + S_n^\alpha(f). \quad (24)$$

But if the only signal with the particular cycle frequency α_k is $T_k(t)$, then as $t \rightarrow \infty$ we have

$$S_T^\alpha = S_{T_k}^\alpha \quad (25)$$

regardless of the temporal or spectral overlap among $\{T_l(t)\}$ and also $n(t)$. This perfect signal selectivity of an ideal cyclic spectral density enables us to detect the presence of signals buried in noise and classify such corrupted signals according to modulation type. This would be impossible if only conventional spectral density (cyclic spectra at $\alpha = 0$) were used. This application will be the subject of a subsequent publication.

Finally, we reiterate here the differences between ordinary Fourier analysis, cyclic spectral analysis, and the temporal empirical orthogonal function (EOF) method. If the process is stationary, the Fourier components for a particular realization of the process will be independent. This makes it especially convenient for an analysis of variance, since variance contributions in different frequency bands add up to give the total variance (there are no cross terms). If the process is cyclostationary, we can also perform a similar kind of analysis with the eigenfunctions of the lagged covariance along the time axis. These functions (the Karhunen–Loeve functions), which are the Fourier basis for a stationary process, have to be recomputed for every shape of lagged covariance function, a tedious and sometimes hopeless undertaking. The appendix gives the basic concepts of the techniques of cyclostationary EOF. We are investigating the usefulness of this approach in a separate study.

Acknowledgments. The authors wish to thank Prof. W. G. Gardner for his careful review and helpful suggestions. We would also thank the anonymous reviewers for their helpful comments on the manuscript. We are grateful for the support of the National Science Foundation (Climate Dynamics Office) and the National Institute for Global Environmental Change (DOE) through its South Central Regional Center at Tulane University.

APPENDIX

Cyclostationary EOFs

A cyclostationary process $T(t)$ can be represented by a set of jointly stationary processes $\{T_l(t): l = 0, \pm 1, \pm 2, \dots\}$ as follows:

$$T(t) = \sum_{l=-d/2}^{d/2} T_l(t) e^{i2\pi lt/d}, \quad (A1)$$

where d is the period of cyclostationarity. The jointly stationary processes, $T_l(t)$, can be expressed as

$$T_l(t) = \int_{-\infty}^{+\infty} w(t - \tau) T(\tau) e^{-i2\pi \tau l/d} d\tau \quad (A2)$$

for which

$$w(t) = \frac{\sin(\pi t/d)}{\pi t}. \quad (A3)$$

This representation is most easily understood in the frequency domain. This representation partitions the frequency support of $T(t)$ into disjoint bands of width $1/d$ centered at integer multiples $\{l/d\}$ of $1/d$, so that the l th component in (26) is simply the response of an ideal bandpass filter.

The l th representor, $T_l(t)$, is the frequency-centered (low-pass) version of the l th component. It follows that there are only a finite number of nonzero representors for a process with finite bandwidth. Although (A1) is a valid representor for any process, it is especially appropriate for a cyclostationary process with period d because then the representors are jointly stationary (Gardner and Franks 1975).

It follows from (A1) that the covariance function for $T(t)$ is represented by

$$C(t, t') = \sum_{l, l' = -d/2}^{d/2} C_{ll'}(t - t') e^{i2\pi(l-l')t'/d}, \quad (\text{A4})$$

where

$$C_{ll'}(t - t') = \langle T_l(t) T_{l'}^*(t') \rangle. \quad (\text{A5})$$

Now we seek the solution of eigenfunction $\Psi(t)$:

$$\int_{-N/2}^{N/2} C(t, t') \Psi(t') dt' = \lambda \Psi(t). \quad (\text{A6})$$

The eigenfunction $\Psi(t)$ can be represented by

$$\Psi_n(t) = \sum_{l = -d/2}^{d/2} \psi_{nl} e^{i2\pi lt/d} e^{i2\pi nt/N}, \quad (\text{A7})$$

where label n corresponds to a kind of Fourier frequency that might be very low compared to $1/d$, which then corresponds to interannual variability. Here N is the length of data. Label l corresponds to a kind of seasonal cycle frequency, which refers to seasonal variability.

After some manipulation, we obtain

$$\sum_l S^{(l-l)/d} \left(f + \frac{l+l'}{2d} \right) \psi_{nl} = \lambda_n \psi_{nl}, \quad (\text{A8})$$

where $S^{l/d}(f)$ is cyclic spectral density. The above suggests that the eigenfunction is easily found if the cyclic spectral density are found in advance. A computationally efficient algorithm based on Bloch's theorem was proposed by North (G. North 1994, unpublished manuscript). This application will be the subject of a subsequent publication.

REFERENCES

- Bennett, W. R., 1958: Statistics of regenerative digital transmission. *Bell. Syst. Tech. J.*, **37**, 1501–1542.
- Bloomfield, P., H. L. Hurd, and R. B. Lund, 1994: Periodic correlation in stratospheric ozone data. *J. Time Ser. Anal.*, **15**, 127–150.
- Gardner, W. A., 1986: The spectral correlation theory of cyclostationary time-series. *Signal Processing*, **11**, 13–36.
- , 1988: *Statistical Spectral Analysis: A Nonprobabilistic Theory*. Prentice Hall, 456 pp.
- , 1994: An introduction to cyclostationary signals. *Cyclostationarity in Communications and Signal Processing*. W. A. Gardner, Ed., IEEE Press, 504 pp.
- , and L. E. Franks, 1975: Characterization of cyclostationary random processes. *IEEE Trans. Inform. Theory*, **21**, 4–14.
- Gladyshev, E. G., 1961: Periodically correlated random sequences. *Sov. Math.*, **2**, 385–388.
- Gutzler, D. S., and R. A. Madden, 1993: Seasonal variations of the 40–50-day oscillation in atmospheric angular momentum. *J. Atmos. Sci.*, **50**, 850–860.
- Hack, J. J., B. A. Boville, B. P. Briegleb, J. T. Kiehl, P. J. Rasch, and D. L. Williamson, 1993: Description of the NCAR Community Climate Model (CCM2). NCAR Tech. Note, NCAR/TN-382+STR, NCAR, Boulder, CO, 108 pp.
- Hasselmann, K., 1976: Stochastic climate model. *Tellus*, **28**, 473–485.
- , and T. P. Barnett, 1981: Techniques of linear prediction for system with periodic statistics. *J. Atmos. Sci.*, **38**, 2275–2283.
- Hurd, H. L., 1969: An investigation of periodically correlated stochastic processes. Ph.D. dissertation, Duke University, 177 pp.
- Jin, F.-F., J. D. Neelin, and M. Ghil, 1994: El Niño on the devil's staircase: Annual subharmonic steps to chaos. *Science*, **264**, 70–72.
- Jones, R. H., 1964: Spectral analysis and linear prediction of meteorological time series. *J. Appl. Meteor.*, **3**, 45–52.
- , and W. M. Brelsford, 1967: Time series with periodic structure. *Biometrika*, **54**, 403–407.
- Lau, N. C., and K. M. Lau, 1986: The structure and propagation of intraseasonal oscillations appearing in a GFDL general circulation model. *J. Atmos. Sci.*, **43**, 2023–2047.
- Leung, L., and G. R. North, 1991: Atmospheric variability on a zonally symmetric all-land planet. *J. Climate*, **4**, 753–765.
- Lund, R. B., H. L. Hurd, P. Bloomfield, and R. Smith, 1995: Climatological time series with periodic correlation. *J. Climate*, **8**, 2787–2809.
- Madden, R. A., 1986: Seasonal variation of the 40–50 day oscillation in the Tropics. *J. Atmos. Sci.*, **43**, 3138–3158.
- , and P. R. Julian, 1971: Detection of a 40–50 day oscillation in the zonal wind in the tropical Pacific. *J. Atmos. Sci.*, **28**, 702–708.
- , and —, 1972: Description of global scale circulation cells in the tropics with 40–50 day period. *J. Atmos. Sci.*, **29**, 1109–1123.
- Markelov, V. A., 1966: Axis crossings and relative time of existence of a periodically nonstationary random process. *Sov. Radiophys.*, **9**, 440–443.
- North, G. R., and R. F. Cahalan, 1981: Predictability in a solvable stochastic climate model. *J. Atmos. Sci.*, **38**, 504–513.
- , K.-Y. Yip, R. Leung, and R. Chervin, 1992: Forced and free variations of the surface temperature field in a GCM. *J. Climate*, **5**, 227–239.
- , R. E. Bell, and J. W. Hardin, 1993: Fluctuation dissipation in a general circulation model. *Climate Dyn.*, **8**, 259–264.
- Ogura, H., 1971: Spectra representation of periodic nonstationary random processes. *IEEE Trans. Inform. Theory*, **17**, 143–149.
- Roberts, R. S., W. A. Brown, and H. H. Loomis Jr., 1994: A review of digital spectral correlation analysis: Theory and implementation. *Cyclostationarity in Communications and Signal Processing*. W. A. Gardner, Ed., IEEE Press, 504 pp.
- Tziperman, E., L. Stone, M. A. Cane, and H. Jaroh, 1994: El Niño chaos: Overlapping of resonances between the seasonal cycle and the Pacific ocean-atmosphere oscillator. *Science*, **264**, 72–74.
- Yip, K.-J., and G. R. North, 1993: Tropical waves in a GCM with zonal symmetry. *J. Climate*, **6**, 1691–1702.
- Zwiers, F., and H. von Storch, 1990: Regime-dependent autoregressive time series modeling of the southern oscillation. *J. Climate*, **3**, 1347–1368.